doi:10.1093/plcell/koab136

THE PLANT CELL

THE PLANT CELL 2021: 33: 2869–2882

Research Article

RAD51 supports DMC1 by inhibiting the SMC5/6 complex during meiosis

Hanchen Chen ,[1,‡] Chengpeng He ,[2,‡] Chongyang Wang ,[1,‡] Xuanpeng Wang ,[1] Fengyin Ruan,[1] Junjie Yan,[1] Ping Yin ,[1] Yingxiang Wang [2,*,†] and Shunping Yan [1,*,†]

1 College of Life Science and Technology, Center of Integrative Biology, Interdisciplinary Science Research Institute, Huazhong Agricultural University, Wuhan 430070, China

2 State Key Laboratory of Genetic Engineering and Ministry of Education, Key Laboratory of Biodiversity Sciences and Ecological Engineering, Institute of Plant Biology, School of Life Sciences, Fudan University, Shanghai 200438, China

*Author for correspondence: spyan@mail.hzau.edu.cn (S.Y.), yx_wang@fudan.edu.cn (Y.W.).

†Senior authors.

These authors contributed equally to this work (H.C., C.H., C.W.).

S.Y. and Y.W. conceived the experiments. H.C., C.H., C.W., X.W., F.R., and J.Y. carried out the experiments. S.Y., Y.W., and P.Y. supervised the project. S.Y., Y.W., and H.C. wrote the paper with inputs from all authors.

The authors responsible for distribution of materials integral to the findings presented in this article in accordance with the policy described in the Instructions for Authors (https://academic.oup.com/plcell) are: Shunping Yan (spyan@mail.hzau.edu.cn) and Yingxiang Wang (yx_wang@fudan.edu.cn).

Abstract

Meiosis is a fundamental process for sexual reproduction in most eukaryotes and the evolutionarily conserved recombinases RADiation sensitive51 (RAD51) and Disrupted Meiotic cDNA1 (DMC1) are essential for meiosis and thus fertility. The mitotic function of RAD51 is clear, but the meiotic function of RAD51 remains largely unknown. Here we show that RAD51 functions as an interacting protein to restrain the Structural Maintenance of Chromosomes5/6 (SMC5/6) complex from inhibiting DMC1. We unexpectedly found that loss of the SMC5/6 partially suppresses the *rad51* knockout mutant in terms of sterility, pollen inviability, and meiotic chromosome fragmentation in a DMC1-dependent manner in *Arabidopsis thaliana*. Biochemical and cytological studies revealed that the DMC1 localization in meiotic chromosomes is inhibited by the SMC5/6 complex, which is attenuated by RAD51 through physical interactions. This study not only identified the long-sought-after function of RAD51 in meiosis but also discovered the inhibition of SMC5/6 on DMC1 as a control mechanism during meiotic recombination.

Introduction

Meiosis is required for sexual reproduction in most eukaryotes. During meiosis, a single round of DNA replication is followed by two rounds of cell division, thus leading to the production of haploid gametes with half the number of chromosomes. After fertilization and the fusion of male and female gametes, the number of chromosomes returns to diploid level, thereby maintaining the same number of chromosomes over different generations. One of the most important events during meiosis is meiotic recombination, through which the homologous chromosomes pair and exchange their genetic information, which consequently ensures the reduction of chromosome numbers and generation of genetic diversity among offspring (Mercier et al., 2015; Wang and Copenhaver, 2018).

Meiotic recombination initiates from the formation of programmed Double-Strand Breaks (DSBs) mediated by the DNA transesterase SPO11 as well as topoisomerase VIB-like

Received January 5, 2021. Accepted May 12, 2021. Advance access publication May 16, 2021

protein (Bergerat et al., 1997; Grelon, 2001; Keeney, 2001; de Massy, 2013; Robert et al., 2016; Vrielynck et al., 2016). These DSBs must be repaired to ensure successful meiosis. Previous studies have shown that the two evolutionarily conserved recombinases RADiation sensitive51 (RAD51) and Disrupted Meiotic cDNA1 (DMC1) are essential to repair these DSBs through the homologous recombination (HR) pathway (Bishop, 1994; Tarsounas et al., 1999; Pradillo et al., 2014; Hinch et al., 2020). Both RAD51 and DMC1 bind to the processed single end of DSBs and facilitate single-strand invasion to search for homologous sequences. Loss of function of either RAD51 or DMC1 results in defective meiosis and sterility in many species, including *Arabidopsis thaliana* (Couteau et al., 1999; Li et al., 2004).

Recent studies in budding yeast (*Saccharomyces cerevisiae*) and Arabidopsis revealed that although RAD51 is essential for meiosis, its recombinase activity is fully dispensable (Cloud et al., 2012; Da Ines et al., 2013). In budding yeast, although the *rad51-II3A* mutant protein lost enzyme activity and was defective in D-loop formation, it rescued the meiotic defects of the *rad51* deletion mutant (Cloud et al., 2012). In Arabidopsis, the RAD51–GFP fusion protein, which lost its DNA break repair capacity in mitotic cells, can fully complement the meiotic chromosomal fragmentation and sterility of the *rad51* knockout mutant (Da Ines et al., 2013). Based on these results, it was concluded that DMC1 is capable of catalyzing the repair of all meiotic DSBs, and RAD51 only plays supporting roles in this process (Cloud et al., 2012; Da Ines et al., 2013). Through in vitro biochemical studies, the budding yeast RAD51 was shown to promote the recombinase activity of DMC1 (Cloud et al., 2012; Chan et al., 2019; Lan et al., 2020). However, it remains to be determined whether this reflects the in vivo function of RAD51 or whether this mechanism is conserved in other organisms, especially in multicellular organisms.

The Structural Maintenance of Chromosomes5/6 (SMC5/6) complex, related to cohesin and condensin, plays multiple essential roles in DSB repair in eukaryotes (Uhlmann, 2016; Aragón, 2018). It is recruited to DSBs and promotes DNA repair through the HR pathway in mitotic and meiotic cells (Pebernard et al., 2006; Fukuda et al., 2013; Verver et al., 2014; Verver et al., 2016; Aragón, 2018). Studies in budding yeast revealed that the SMC5/6 complex is required to prevent the accumulation of DNA intermediates by inhibiting the formation of DNA intermediates and facilitating the resolution of recombination intermediates (Wehrkamp-Richter et al., 2012; Copsey et al., 2013; Lilienthal et al., 2013; Xaver et al., 2013). The SMC5/6 complex contains SMC5, SMC6, and six non-SMC elements (NSE1–NSE6). Except NSE5 and NSE6, all the other components are highly conserved in all eukaryotes (Potts, 2009; Wang et al., 2018). Functional homologs of the NSE5 and NSE6 subunits have been identified in budding yeast, fission yeast (*Schizosaccharomyces pombe*), Arabidopsis, and humans (Hazbun et al., 2003; Pebernard et al., 2006; Yan et al., 2013; Raschle et al., 2015). In Arabidopsis, Suppressor of NPR1-1, Inducible 1 (SNI1) and its interacting protein Arabidopsis SNI1-Associated Protein 1 (ASAP1) were identified as functional homologs of NSE6 and NSE5, respectively (Yan et al., 2013). Genetic studies revealed that loss of function of RAD51 could suppress the stunted growth of *sni1* and *asap1* mutants, suggesting that the SMC5/6 complex negatively regulates RAD51 in mitosis (Wang et al., 2010; Yan et al., 2013). Recently, the NSE4 subunit was found to be involved in meiosis and seed development in Arabidopsis (Díaz et al., 2019; Zelkowski et al., 2019). Despite the importance of SMC5/6 and RAD51/DMC1 in meiosis, their functional relationships are still unknown.

In this study, we unexpectedly found that loss of SMC5/6 could partially suppress the sterility of the *rad51* knockout mutant in a DMC1-dependent manner. Cytological studies suggested that DMC1 localization in meiotic chromosomes is inhibited by SMC5/6. Biochemical studies revealed that RAD51, DMC1, ASAP1, and SNI1 interact with each other, and RAD51 attenuates the interaction between DMC1 and ASAP1/SNI1, suggesting that RAD51 supports DMC1 by inhibiting the SMC5/6 complex. Our study thus uncovers the supporting role of RAD51 in meiosis and provides evidence that DMC1 is inhibited by SMC5/6.

Results

Loss of function of the SMC5/6 complex partially suppresses the sterility and pollen inviability of the *rad51* mutant

As a subunit of the SMC5/6 complex, ASAP1 is required for plant development and loss of function of ASAP1 causes severe growth defects in Arabidopsis (Yan et al., 2013). Previously, it was found that loss of function of RAD51 partially suppressed the growth retardation of the *asap1* knockout mutant (Yan et al., 2013). Unexpectedly, we found the *asap1* mutant also partially suppressed the sterility of the *rad51* knockout mutant. As shown in Figure 1, A–C, the silique length and seed number in the *rad51 asap1* double mutant were significantly higher than those in either *asap1* or *rad51* single mutants. Since SNI1 interacts with ASAP1 to form a subcomplex in the SMC5/6 complex, it was expected that loss of function of SNI1 could also suppress *rad51*.

However, the *rad51 sni1-1* double mutant was still completely sterile (Supplemental Figure S1). One explanation was that the *sni1-1* mutant is caused by a point-mutation (Li et al., 1999) and the mutated protein is partially functional. To test this possibility, we crossed *rad51* with the *sni1-2* mutant, which contains a T-DNA insertion in the coding region of *SNI1* and lacks detectable expression of *SNI1* (Supplemental Figure S2). Consistent with the hypothesis, the resulting *rad51 sni1-2* double mutant was indeed partially fertile, resembling the *rad51 asap1* double mutant (Figure 1, A–C). Methyl Methane Sulfonate Sensitivity 21 (MMS21) is the NSE2 subunit of SMC5/6 and has also a role in meiosis (Xaver et al., 2013; Liu et al., 2014). Consistent with this, loss of function of MMS21 also partially suppressed the sterility of *rad51* (Supplemental Figure S3).

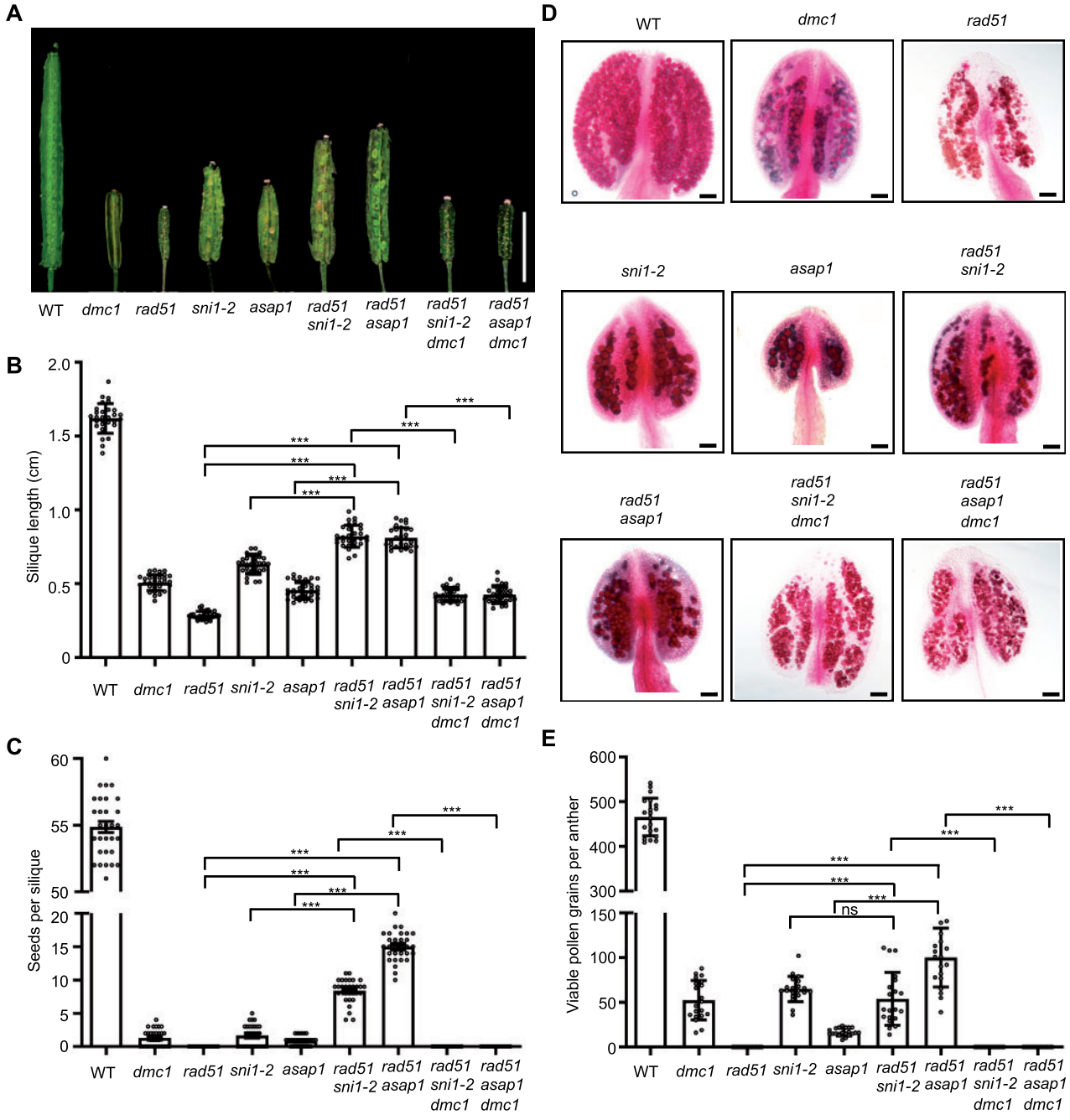

Figure 1 Loss of function of SMC5/6 partially suppresses fertility and pollen inviability of the *rad51* mutant in a DMC1-dependent manner. A, The representative pictures of siliques of WT, *dmc1*, *rad51*, *sni1-2*, *asap1*, *rad51 sni1-2*, *rad51 asap1*, *rad51 sni1-2 dmc1*, and *rad51 asap1 dmc1*. Bar = 0.5 cm. A total of 30 siliques from different plants per genotype were examined. B, The length of siliques. C, The seed numbers per silique. The data in (B) and (C) are represented as means ± SD ($n = 30$). The statistical significance was determined by Student's *t* test (two-tailed; ***$P < 0.001$). D, Representative images of Alexander staining of pollen. Red was viable, dark blue or purple were dead. Bar = 50 μm. A total of 20 siliques from different plants per genotype were examined. E, Quantification of viable pollen grains per anther. The data are represented as means ± SD ($n = 20$). The statistical significance was determined by Student's *t* test (two-tailed; ns, not significant; ***$P < 0.001$)

Together, the genetic data provided strong evidence that loss of function of the SMC5/6 complex partially suppresses the sterility of *rad51*, suggesting that the function of RAD51 in meiosis is to inhibit the SMC5/6 complex.

It was suggested that DMC1 is the recombinase that performs meiotic recombination (Cloud et al., 2012; Da Ines et al., 2013). The partially restored fertility in the *rad51 asap1* and *rad51 sni1-2* double mutants indicated that

DMC1 is functional in these mutants. To test this possibility, we investigated whether the restored fertility in *rad51 asap1* and *rad51 sni1-2* is dependent on DMC1. We obtained the *rad51 asap1 dmc1* and *rad51 sni1-2 dmc1* triple mutants by crossing the double mutants with the *dmc1*$^{+/-}$. As expected, the triple homozygous mutant was completely sterile, similar to the *rad51* single mutant (Figure 1, A–C), supporting the idea that the remained fertility in both *rad51 asap1* and *rad51 sni1-2* double mutants is DMC1-dependent.

Previous studies showed that the pollen in *rad51* is completely inviable (Li et al., 2004). To investigate whether pollen viability is also restored in these double mutants, Alexander staining was performed to examine the pollen viabilities (Figure 1D). Consistent with fertility phenotypes, the pollen grains in the *rad51* mutant were completely inviable (Figure 1, D and E). The pollen inviability was partially suppressed in the *rad51 asap1* and *rad51 sni1-2* double mutants, but was recaptured in the *rad51 asap1 dmc1* and *rad51 sni1-2 dmc1* triple mutants (Figure 1, D and E).

Loss of function of the SMC5/6 complex partially suppresses meiotic chromosome morphology defects in *rad51*

Our genetic data suggested that SNI1 and ASAP1 are involved in meiosis. To further characterize their roles in meiosis, we performed chromosome spreads with 4′,6-diamidino-2-phenylindole (DAPI) staining. As shown in Figure 2, in wild-type (WT, $n = 29$) pachytene meiocytes, homologous chromosomes fully synapsed and formed thick thread-like chromosomes. The *sni1-2* ($n = 91$) and *asap1* ($n = 80$) pachytene meiocytes displayed normal pachytene-like chromosomes, which were obviously distinguishable to the *rad51* ($n = 29$) pachytene meiocytes lacking synapsis. At diakinesis, five bivalents are observed in both *sni1-2* and *asap1*. At subsequent metaphase I and anaphase I, chromosome fragments are observed in *sni1-2* and *asap1*, which may result from the abnormal resolution of recombination intermediates. Intriguingly, the *rad51 asap1* ($n = 20$) and *rad51 sni1-2* ($n = 20$) double mutants displayed restored pachytene chromosomes and reduced chromosome fragments, similar to either *sni1-2* or *asap1* (Figure 2). Moreover, both the *rad51 asap1 dmc1* ($n = 49$) and *rad51 sni1-2 dmc1* ($n = 92$) triple mutants resembled *rad51* single mutant in pachytene chromosomes and chromosome fragmentation (Figure 2).

To examine the number of chromosome fragments in the *rad51 asap1* and *rad51 sni1-2* double mutants, we performed chromosome fluorescence in situ hybridization (FISH) with labeled centromere 180-bp repeats as the probe. As shown in Figure 3, in *rad51* ($n = 33$), there were many small-sized fragments, which make it infeasible to count an accurate number (Figure 3A). Therefore, we defined the number of fragments a range of >10 in *rad51* (Figure 3B). In the other mutant background, we only counted the lagged broken chromosomes that were large in size. Compared with *rad51*, the *rad51 asap1* ($n = 65$) and *rad51 sni1-2* ($n = 23$) double mutants showed significantly reduced chromosome fragments (Figure 3, A and B). However, the fragments in the *rad51 asap1 dmc1* ($n = 25$) and *rad51 sni1-2 dmc1* ($n = 27$) triple mutants resembled that of *rad51* (Figure 3, A and B). Together, these results also support the idea that loss of function of SMC5/6 suppresses chromosome fragmentation in *rad51* in a DMC1-dependent manner. These data further suggested that DMC1 is partially functional to repair DSBs in the *rad51 asap1* and *rad51 sni1-2* mutants, supporting the possibility that DMC1 is inhibited by the SMC5/6 complex.

Loss of function of the SMC5/6 complex restores synapsis and the DMC1 foci in *rad51*

The chromosome spread of *rad51 sni1-2* and *rad51 asap1* had pachytene-like chromosomes (Figure 2), indicating that synapsis is restored in these mutants compared with *rad51*. To test this hypothesis, we analyzed the axial element proteins Asynaptic1 (ASY1; Armstrong et al., 2002) and transverse filament component ZIPPER1 (ZYP1; Higgins et al., 2005) of synaptonemal complex. In WT zygotene meiocytes, ASY1 formed continuous signals and ZYP1 had discrete signals ($n = 11$). Following full synapsis at pachytene, ASY1 was gradually removed from chromosomes to remain a discrete signal, while ZYP1 formed a continuous signal overlapping with chromosomes ($n = 29$, Figure 4). In contrast, the *rad51* single mutant showed normal ASY1 signals, but lacked ZYP1 signals at similar stage ($n = 39$) due to the absence of synapse (Figure 4). Consistent with chromosome morphology, as shown by DAPI staining (Figure 2), there was no apparent difference of synapsis between WT, *sni1-2* (zygotene: $n = 30$, pachytene: $n = 46$), *asap1* (zygotene: $n = 28$, pachytene: $n = 35$), *rad51 sni1-2* (zygotene: $n = 49$, pachytene: $n = 45$), and *rad51 asap1* (zygotene: $n = 32$, pachytene: $n = 28$; Figure 4). These data support the idea that synapsis appears normal in *sni1* and *asap1*, and mutations of *SNI1* and *ASAP1* restore the absent synapsis in *rad51*.

To examine whether the synapsed chromosomes are homologous chromosomes in *sni1-2*, *asap1*, *rad51 sni1-2*, and *rad51 asap1*, we performed chromosome painting by labeling the entire Chromosome 1 as a probe. In WT pachytene meiocytes, two homologous Chromosome 1 paired and synapsed. We observed a thread-like signal overlapping with chromosome (Supplemental Figure S4A), indicating a full synapsis. Similar Chromosome 1 signals were also observed in *sni1-2*, *asap1*, *rad51 sni1-2*, and *rad51 asap1* mutants (Supplemental Figure S4A). Furthermore, we analyzed the 45S rDNA pairing at zygotene and pachytene meiocytes and found that the signals in *sni1-2*, *asap1*, *rad51 sni1-2*, and *rad51 asap1* mutants were indistinguishable to WT (Supplemental Figure S4B).

Previous studies suggested that DMC1 is capable of catalyzing the repair of all meiotic DSBs (Cloud et al., 2012; Da Ines et al., 2013). The sterility of *rad51* was partially restored in *rad51 sni1-2* and *rad51 asap1*, indicating that DMC1 is

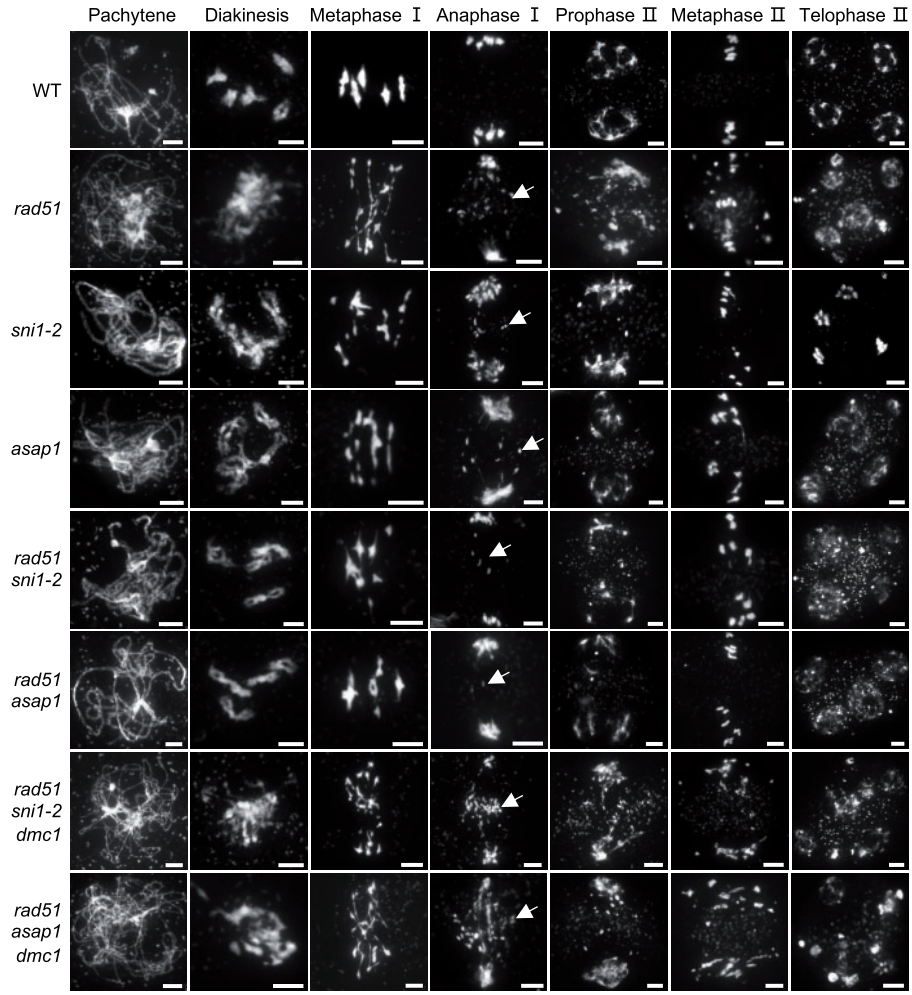

Figure 2 Chromosomes morphologies stained with DAPI. Representative image showing meiotic chromosome feature of WT, *rad51*, *sni1-2*, *asap1*, *rad51 sni1-2*, *rad51 asap1*, *rad51 sni1-2 dmc1*, and *rad51 asap1 dmc1* at specific stages labeled in each panel above. The arrows indicate chromosome fragments. Bar = 5 μm. At least 10 meiocytes from different plants per genotype were examined

functional in *rad51 sni1-2* and *rad51 asap1*. To test this possibility, we performed dual-immunofluorescence using anti-DMC1 and anti-ZYP1 antibodies (Figure 5). Consistent with previous findings (Vignard et al., 2007), the number of DMC1 foci at *rad51* ($n = 25$) zygotene meiocytes significantly decreased compared with WT ($n = 24$; Figure 5, A and B). Interestingly, the number of DMC1 foci significantly increased in the *sni1-2* ($n = 28$) and *asap1* ($n = 24$) mutants compared with WT (Figure 5, A and B). More interestingly, compared with *rad51*, the number of DMC1 foci was dramatically increased in the *rad51 sni1-2* ($n = 31$) and *rad51 asap1* ($n = 22$) mutants (Figure 5, A and B).

To test whether the increase of DMC1 foci in *sni1-2* and *asap1* mutant resulted from the increase of DSB formation, we performed immunofluorescence assays using anti-γ-H2AX (phosphorylated histone H2AX, a DSB indicator) with ZYP1. We found that the numbers of γ-H2AX foci did not differ significantly in *sni1-2*, *asap1*, and *rad51* compared with WT ($n \geqq 25$, Figure 5, C and D). These results indicated that RAD51 promotes DMC1 localization in meiotic chromosomes, while the SMC5/6 complex inhibits it during meiotic recombination.

DMC1, RAD51, and SMC5/6 interact with each other both in vitro and in vivo

To further study the relationship between SMC5/6 and DMC1/RAD51, we tested the physical interactions between ASAP1, SNI1, RAD51, and DMC1. First, we performed in vitro pull-down assays. As shown in Figure 6, A and B, the recombinant RAD51-His and DMC1-His proteins could be pulled down by either GST-ASAP1 or GST-SNI1, but not the GST control. The DMC1-His could also be pulled down specifically by GST-RAD51 (Figure 6C). To test whether these proteins interact in vivo, we performed split-luciferase assays (Figure 6D). The proteins were either fused with the N-terminal half (Nluc) or C-terminal half (Cluc) of firefly luciferase and were transiently co-expressed in *Nicotiana benthamiana*. The interaction was indicated by the luminescence captured by a Charge-Coupled Device (CCD) camera. In line with the in vitro pull-down results, we found that

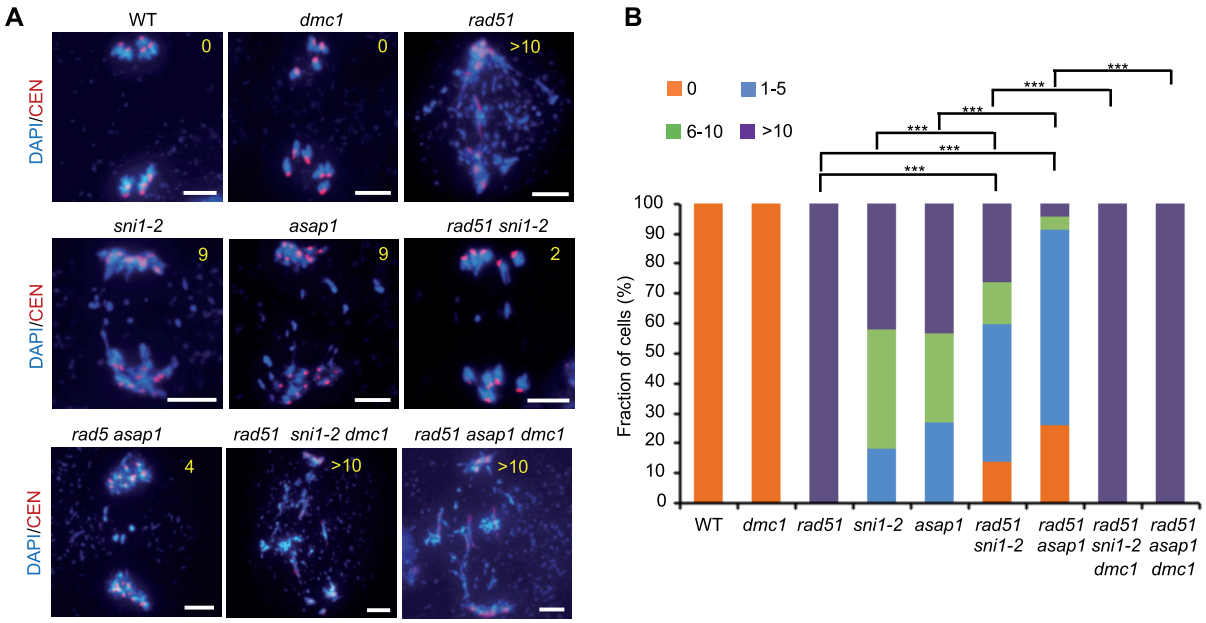

Figure 3 Loss of function of SMC5/6 partially suppresses the chromosome fragmentation of the *rad51* mutant in a DMC1-dependent manner. A, Representative meiotic chromosomes in anaphase I of WT, *dmc1*, *rad51*, *sni1-2*, *asap1*, *rad51 sni1-2*, *rad51 asap1*, *rad51 sni1-2 dmc1*, and *rad51 asap1 dmc1* observed by chromosome spread with centromere FISH. Yellow Arabic number in each image showing the number of chromosome fragments. Blue color refers to the DAPI stained chromosomes. The red dots refer to the centromere signals. Bar = 5 μm. At least 23 meiocytes from different plants per genotype were examined. B, The percentage of cells with different number of chromosome fragments. Four levels of chromosome fragmentation (0, 1–5, 6–10, >10) were used according to the number of chromosome fragments per cell. The statistical significance was determined by Chi-squared test (two-tailed; ***$P < 0.001$)

ASAP1 and SNI1 interact with DMC1 and RAD51, and DMC1 interacts with RAD51. These in vivo interactions were further confirmed by Co-immunoprecipitation (CoIP) assays in Arabidopsis protoplasts (Figure 6, E–G). The RAD51-HA and DMC1-HA proteins were co-immunoprecipitated by either ASAP1-GFP or SNI1-GFP, but not GFP control. The DMC1-HA protein was also co-immunoprecipitated by RAD51-GFP. Together with the reported interaction between ASAP1 and SNI1 (Yan et al., 2013), our results revealed that ASAP1, SNI1, RAD51, and DMC1 can interact with each other both in vitro and in vivo.

RAD51 attenuates the interaction between DMC1 and SMC5/6

Our genetic data suggested that RAD51 negatively regulates SMC5/6 and SMC5/6 inhibits DMC1. Given that DMC1, RAD51, ASAP1, and SNI1 interact with each other, we hypothesized that RAD51 may support DMC1 by attenuating the interaction between DMC1 and SMC5/6. To test this hypothesis, we performed competing pull-down assays. We added the same amount of the GST-SNI1 or GST-ASAP1 and HisMBP-DMC1 proteins but different amounts of RAD51-His in the reaction. As shown in Figure 7, A and B, the amount of GST-SNI1 or GST-ASAP1 pulled down by HisMBP-DMC1 decreased with increasing amounts of RAD51-His. To test whether the competition occurs in vivo, we performed split-luciferase assays. Compared with the empty vector control, when RAD51 was co-expressed with SNI1-Nluc and Cluc-DMC1, the luminescence signal was dramatically reduced (Figure 7C), indicating the interaction between SNI1 and DMC1 is attenuated by RAD51. A similar result was obtained for the RAD51–ASAP1–DMC1 interaction (Figure 7D). Reverse transcription quantitative polymerase chain reaction (RT-qPCR) analyses showed that the decreased luminescence was not because the expression of SNI1-Nluc, ASAP1-Nluc, and Cluc-DMC1 was reduced (Supplemental Figure S5). Although the protein interactions were tested in vitro or in somatic cells, together with our genetic data, we believed that they could reflect the situations in meiotic cellular context.

Discussion

It was suggested that RAD51 and DMC1 bind to the opposite sites of a meiotic DSB in Arabidopsis (Vignard et al., 2007; Kurzbauer et al., 2012). Together with our genetic and biochemical data, we proposed a simplified working model to illustrate how SMC5/6, DMC1, and RAD51 function during meiosis (Figure 8). In WT, the interactions among SMC5/6, RAD51, and DMC1 are balanced, which allows RAD51 and DMC1 to be loaded at the opposite end of DSB sites, thus resulting in successful strand invasion between homologous chromosomes and DSB repair. In the *rad51*

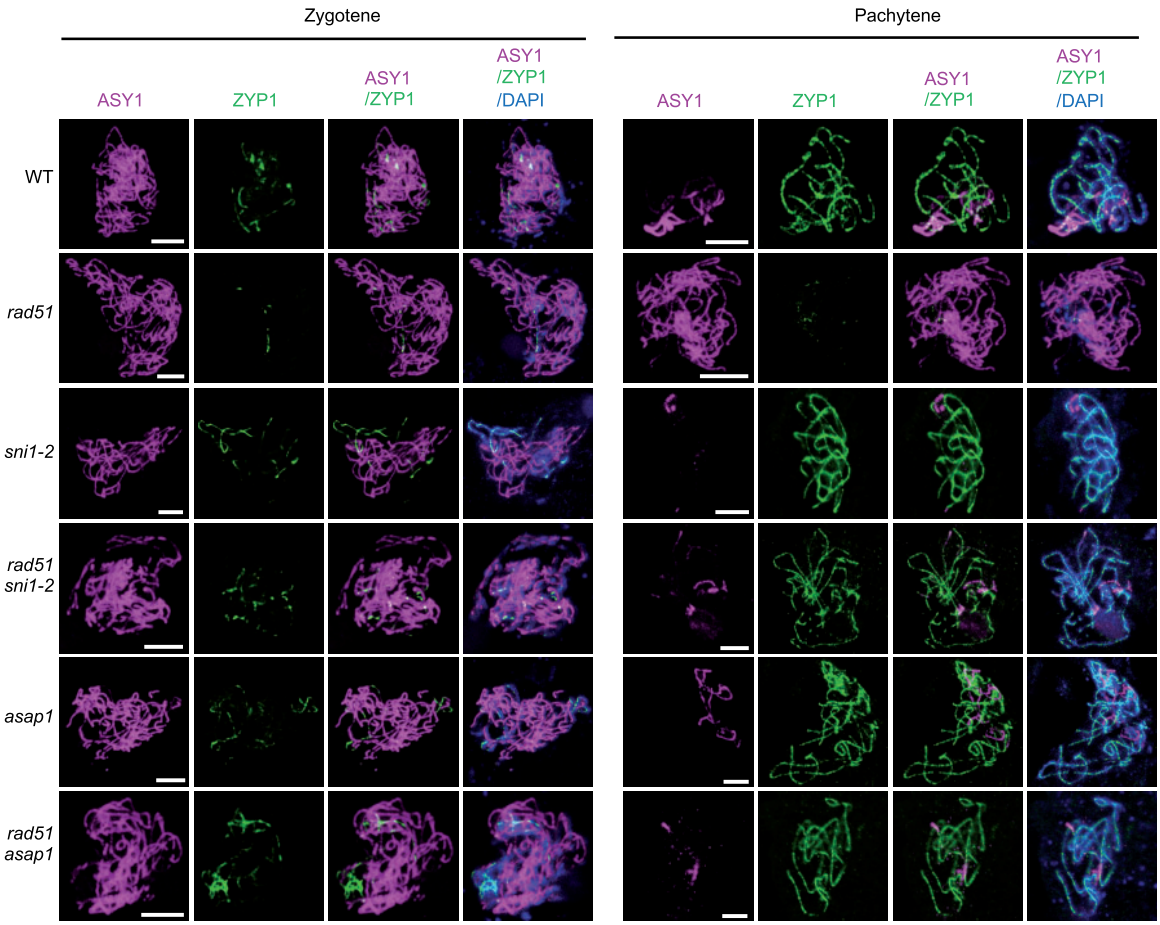

Figure 4 Dual immunostaining of the ASY1 and ZYP1 of synaptonemal complex in zygotene and pachytene meiocytes of WT, *rad51*, *sni1-2*, *rad51 sni1-2*, *asap1*, and *rad51 asap1*. In both panels of zygotene and pachytene meiocytes, the left column in magenta refers to the ASY1 signals, the second column in green refers to the ZYP1 signals, the third column merges the left two columns, and the right column merges the ASY1, ZYP1, and DAPI stained chromosomes. Bar = 5 μm. At least 11 meiocytes from different plants per genotype were examined

mutant, in the absence of RAD51, SMC5/6 interacts with DMC1 to inhibit its binding to single-strand end, thereby preventing strand invasion and DSB repair, subsequently leading to severe chromosome fragmentation and complete sterility. In the *rad51 smc5/6* double mutant, the inhibition of SMC5/6 on DMC1 is abolished, which allows DMC1 to bind to both DSB ends, thereby resulting in successful strand invasion. In the *rad51 smc5/6 dmc1* triple mutant, since the recombinase is absent, no strand invasion and DSB repair occur, leading to severe chromosome fragmentation and sterility. It is of note that SMC5/6 also functions with resolvases to facilitate the resolution of double Holliday junctions (Pebernard et al., 2006; Xaver et al., 2013; Copsey et al., 2013). Therefore, although the strand invasion is successful in the *rad51 smc5/6* double mutant, the resolution of double Holliday junctions is compromised, which results in partial DSB repair and partial fertility.

The recombinases RAD51 and DMC1 are two key players in meiotic recombination. The relationship between RAD51 and DMC1 is an interesting and important question under extensive study. It was reported that RAD51 is expressed both in mitotic cells and meiotic cells, and DMC1 is only expressed in meiotic cells (Pradillo et al., 2014). Given the presence of meiosis-specific recombinases DMC1, it remains unclear why RAD51 is also essential for meiotic recombination. Recent studies revealed that the enzyme activity of RAD51 is not required for its function in meiosis (Cloud et al., 2012; Da Ines et al., 2013), suggesting that cells evolved to use RAD51 as a non-enzyme protein during meiosis. However, the exact function of RAD51 in meiosis is unclear. Our study suggested that RAD51 functions as an interacting protein of SMC5/6 and DMC1 to support DMC1 to bind DSBs. RAD51 may attenuate the interaction between SMC5/6 and DMC1 in two ways. On the one hand, RAD51 interacts with SMC5/6 to reduce the capacity of SMC5/6 in binding DMC1. On the other hand, RAD51 interacts with DMC1 to prevent DMC1 from being bound by SMC5/6. In this regard, RAD51 functions as a "brake" of SMC5/6 and a "protector" of DMC1.

Unrestrained recombination causes undesired consequences such as translocation, deletion, inversion, and the

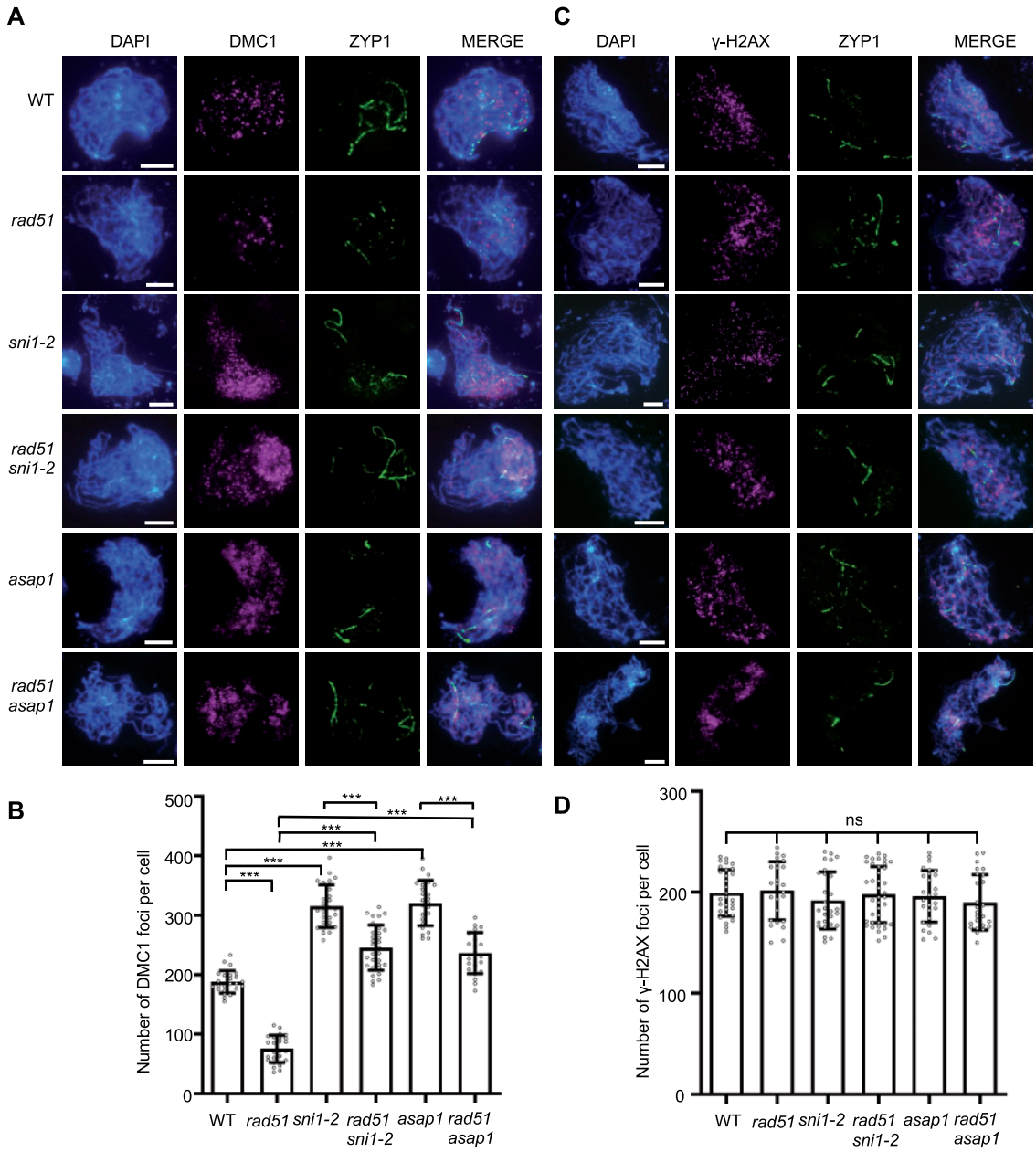

Figure 5 Loss of function SMC5/6 restores the DMC1 foci in *rad51* mutant. A, The colocalization of DMC1 and ZYP1 in zygotene meiocytes of WT, *rad51*, *sni1-2*, *rad51 sni1-2*, *asap1*, and *rad51 asap1*. Bar = 5 μm. At least 22 meiocytes from different plants per genotype were examined. B, Quantification of DMC1 foci per cell. The data are represented as means ± SD ($n \geqq 22$). The statistical significance was determined by Student's *t* test (two-tailed; ***$P < 0.001$). C, The colocalization of γ-H2AX and ZYP1 in zygotene meiocytes of WT, *rad51*, *sni1-2*, *rad51 sni1-2*, *asap1*, and *rad51 asap1*. Bar = 5 μm. At least 25 meiocytes from different plants per genotype were examined. D, Quantification of γ-H2AX foci per cell. The data are represented as means ± SD ($n \geqq 25$). The statistical significance was determined by Student's *t* test (two-tailed; ns, not significant)

accumulation of toxic recombination intermediates (Heyer et al., 2010). Recently, it was reported that in the gain-of-function *dmc1* mutant in budding yeast (*S. cerevisiae*), *dmc1-E157D*, recombination is abnormal because it displays unusually high levels of multi-chromatid and inter-sister joint molecule intermediates, as well as high levels of ectopic recombination products (Reitz et al., 2019). Therefore, the activity of DMC1 must be precisely regulated. However, how DMC1 is restrained is not well-understood. It has been shown that SMC5/6 is required to exclude RAD51 to prevent abnormal recombination in mitotic cells (Chiolo et al., 2011). In this study, our genetic and biochemical data suggested that SMC5/6 inhibits DMC1 binding to DSBs. Therefore, our study not only reveals the supporting function of RAD51 in meiosis but also uncovers a negative regulation mechanism of DMC1. Since SMC5/6, DMC1, and

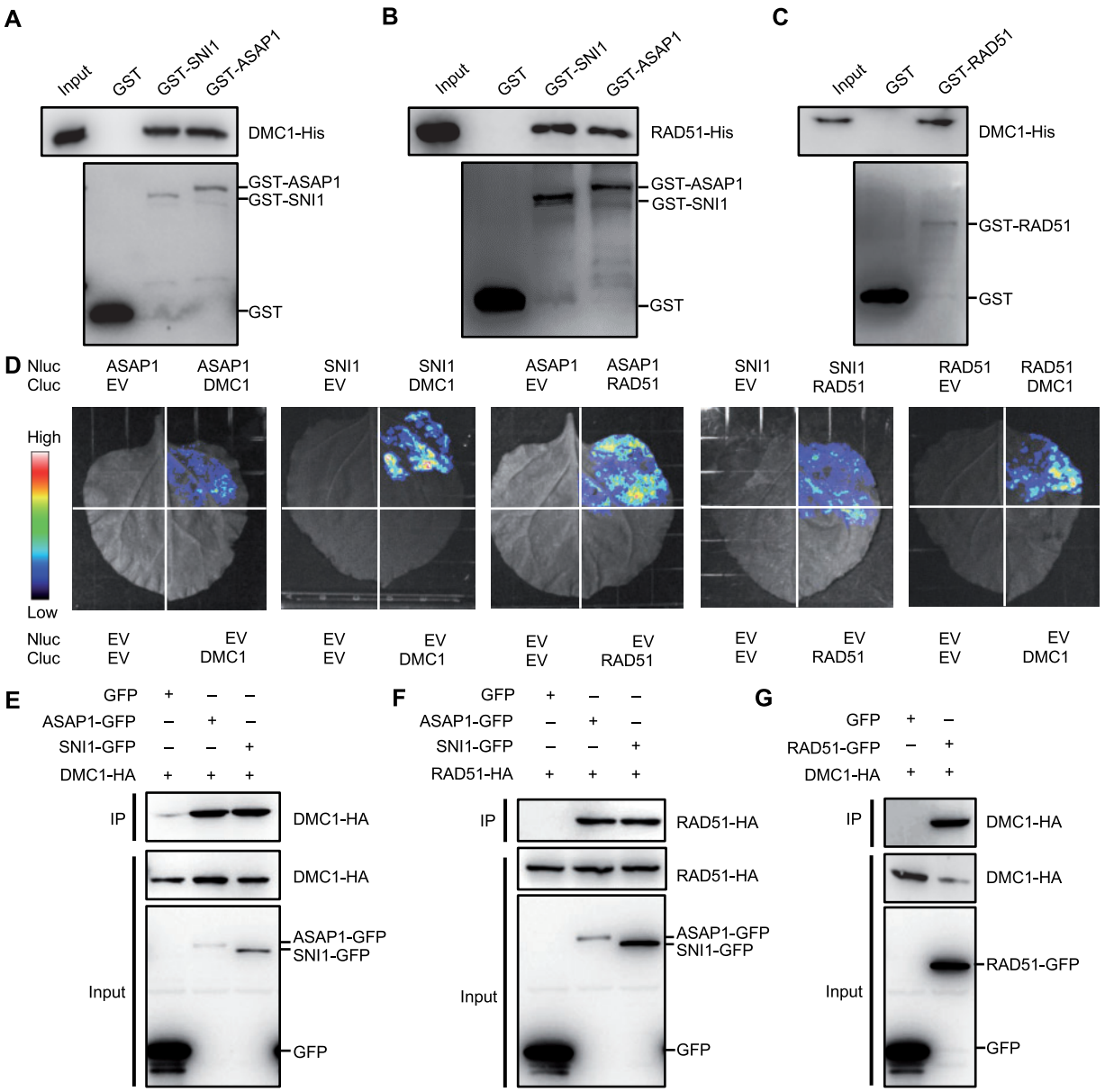

Figure 6 DMC1, RAD51, ASAP1, and SNI1 interact with each other. A–C, In vitro pull-down assays. The recombinant GST, GST-SNI1, GST-ASAP1, or GST-RAD51 proteins were coupled to glutathione beads and incubated with the recombinant DMC1-His or RAD51-His proteins. After washing, the beads were subjected to western blotting using anti-His or anti-GST antibodies. The experiments were repeated three times using different batches of proteins with similar results. D, Split luciferase assays. The Agrobacterium bacteria carrying the indicated constructs were co-expressed in *N. benthamiana* leaves. The positive luminescence detected by a CCD camera indicates interaction. EV, empty vector. Nluc, N-terminal luciferase. Cluc, C-terminal luciferase. The experiments were repeated three times using leaves from different plants with similar results. E–G, CoIP assays. DMC1-HA or RAD51-HA was co-expressed with GFP, SNI1-GFP, ASAP1-GFP, or RAD51-GFP in Arabidopsis protoplasts. Immunoprecipitation was performed using GFP-Trap beads and western blotting was performed using anti-HA or anti-GFP antibodies. The experiments were repeated three times using proteins from independent transfection with similar results

RAD51 are highly conserved in eukaryotes, it will be interesting to investigate whether these mechanisms are conserved in other organisms.

Materials and methods

Plant materials and growth conditions

All *A. thaliana* mutants except *dmc1* (in *Wassilewskaja* background) used in this study were in *Columbia-0* background. The mutants of *rad51* (GABI_134A01), *sni1-2* (SAIL_298_H07), and *asap1* (GABI_218F01) were purchased from the Arabidopsis Biological Resource Center (https://abrc.osu.edu). The *dmc1*, *sni1-1*, and *mms21* mutants were described previously (Couteau et al., 1999; Huang et al., 2009; Li et al., 1999). Seeds were sterilized with 2% Plant Preservative Mixture-100 (Plant Cell Technology) and stratified at 4°C in the dark for 2 days, and then were plated on Murashige and Skoog medium with 1% sucrose and 0.3%

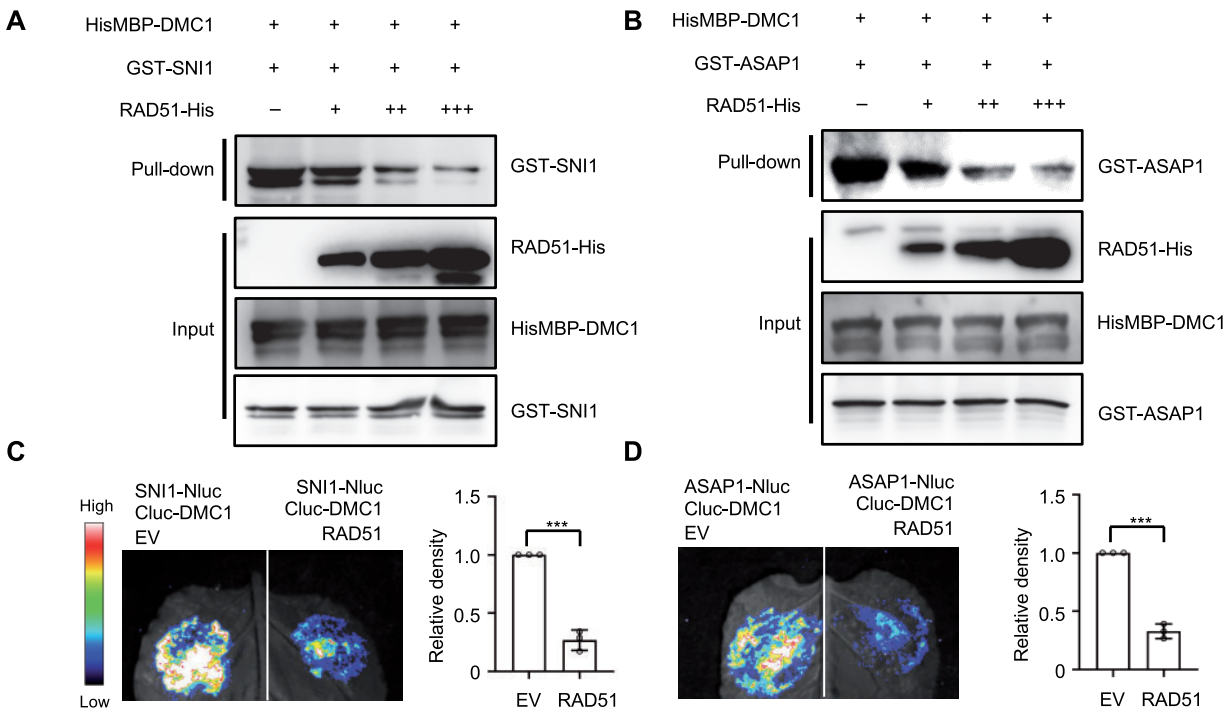

Figure 7 RAD51 attenuates the interaction between DMC1 and SMC5/6. A, B, In vitro pull-down assays. The HisMBP-DMC1 proteins coupled with amylose resin beads were incubated with the same amount of GST-SNI1 or GST-ASAP1 proteins but different amounts of RAD51-His proteins. After washing, the beads were subjected to western blotting using anti-His, anti-GST, or anti-MBP antibodies. –, no GST-RAD51. +, ++, and +++ indicated 1, 2, or 3 volume of GST-RAD51. The experiments were repeated three times using different batches of proteins with similar results. C, D, Split luciferase assays. The Agrobacterium bacteria carrying the indicated constructs were co-expressed in *N. benthamiana* leaves. Nluc, N-terminal luciferase. Cluc, C-terminal luciferase. EV, empty vector. The density of luminescence was quantified using Image J. The relative density to EV group in each leaf ($n = 3$) was calculated. The data are represented as means ±SD ($n = 3$). The statistical significance was determined by Student's *t* test (two-tailed; $^{***}P < 0.001$). The experiments were repeated three times using leaves from different plants with similar results

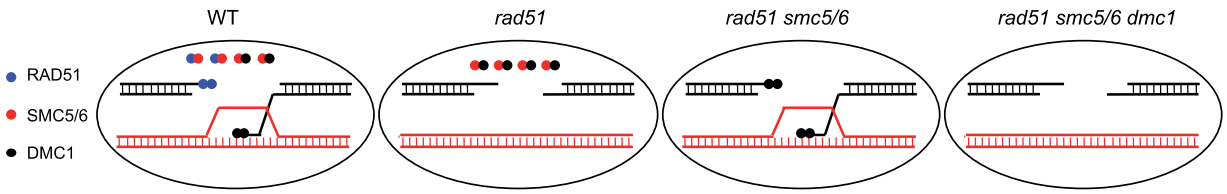

Figure 8 A simplified working model. SMC5/6, RAD51, and DMC1 can interact with each other. SMC5/6 interacts with DMC1 to inhibit its binding to DSBs. RAD51 attenuates the interaction between SMC5/6 and DMC1. In WT, the interactions between SMC5/6, RAD51, and DMC1 are balanced, which allows RAD51 and DMC1 to be loaded at the opposite end of DSB sites, thus resulting in successful strand invasion. In the *rad51* mutant, SMC5/6 interacts with DMC1 to inhibit its binding to DSB, no strand invasion occurring. In the *rad51 smc5/6* double mutant, the inhibition of SMC5/6 on DMC1 is abolished, which allows DMC1 to bind to both DSB ends, thereby resulting in successful strand invasion. In the *rad51 smc5/6 dmc1* triple mutant, in the absence of recombinase, no strand invasion occurs

phytagel. The plants were grown under long-day conditions (16 h of light and 8 h of dark; light intensity is 100 µmol photons m^{-2} s^{-1}; supplied by white-light tubes) at 22°C.

Alexander staining

Alexander staining was performed as described previously (Alexander, 1969). Briefly, the inflorescences were fixed in Carnoy's fixative solution (ethanol: glacial acetic acid = 3:1) and appropriate anthers were separated with Alexander staining solution for 30 min (65°C). Images were captured using Zeiss Axio Scope A1.

Chromosome spreading and centromere FISH

Chromosome spreading and centromere FISH were performed as described previously with minor modifications (Wang et al., 2014). The inflorescences were fixed in Carnoy's fixative solution and the unopen flowers were digested with enzyme mix (3% cellulose, 3% Macerozyme,

5% Snailase) at 37°C for 20 min. After staining with DAPI, the images were captured using Zeiss Axio Scope A2. To quantify the severity of chromosome fragmentation, the number of cells with 0, 1–5, 6–10, and over 10 fragments were determined.

Immunostaining

For immunostaining, the inflorescences were fixed in 2% (v/m) polyformaldehyde for 4–8 h. Stages 4–7 anthers in unopen flowers were separated and digested with enzyme mix (3% cellulose, 3% macerozyme, 5% snailase) at 37°C for 30 min. Slides with proper anthers were immersed in wash buffer (1×phosphate buffered solution, 0.2% Triton) for 1 h at room temperature and blocked with goat serum (Bosterbio) for 30 min before adding anti-ASY1 (rabbit-sourced, 1:200; Wang et al., 2020), anti-ZYP1 (rabbit-sourced, 1:100; Wang et al., 2020), anti-γ-H2AX (rabbit-sourced, 1:400; Huang et al., 2015), and anti-DMC1 (rabbit-sourced, 1:400; Yao et al., 2020) antibodies. Secondary antibodies (Alexa Fluor 555 goat anti-rabbit, A21428; Alexa Fluor 488 goat anti-mouse, A11001; Alexa Fluor 488 goat anti-rabbit, A11008; Alexa Fluor 488 goat anti-rat, A11006; Alexa Fluor 555 goat anti-mouse, A21424; Thermo Fisher) were diluted at 1:750. Images were captured using Zeiss Axio Scope A1 or a Zeiss-LSM880 microscope.

Chromosome 1 painting and 45S rDNA FISH

Chromosome 1 painting was performed using oligonucleotide probes. The probes were selected according to the published paper (Han et al., 2015). Probes were synthesized by Daicel Arbor Biosciences and were labeled following the manufacture manual (Daicel Arbor Biosciences). After labeling by rhodamine, the probes were diluted by hybridization mix and incubating at 37°C for 24 h. Slides were washed 3 times with 2 × SSC for 10 min at room temperature. When slides were air-dried, 8-μL Vectashield mounting medium with DAPI was added to a slide. Chromosome images were captured using a Zeiss Axio Scope A2 microscope.

The FISH was performed as previously described (Lysak et al., 2006) with some modifications. Slides of chromosome spreads were denatured at 85°C for 5 min, rinsed for 5 min in cold 70% (v/v) ethanol, and in 100% ethanol for another 5 min at room temperature. Probes were labeled using DIG-nick translation mix (11745816910, Roche) according to manufacturer's manual. After incubating probes for 95 min at 15°C, 1-μL 0.5 M Ethylene Diamine Tetraacetie Acid (EDTA,PH 8.0) was added to stop the reaction, and the mix was heated to 65°C for 10 min. Slides were completely air-dried, and 1 μL of probe was diluted to 20 μL using hybridization mix. Slides were incubated for 16 h at 37°C, rinsed three times in 2 × SSC for 5 min at room temperature, and blocked for 1 h using goat serum (AR0009, BOSTER) at room temperature. Then, 30 μL of diluted anti-digoxigenin–rhodamine, Fab fragments (Roche, final concentration is 1 $\mu g \cdot mL^{-1}$, diluted by goat serum) was applied to the slide and incubated for 1 h at 37°C. Slides were washed three times with 2 × SSC for 5 min at room temperature. DAPI staining was performed using Vectashield mounting medium DAPI (Vector Laboratories).

Construction of plasmids

The vectors were constructed using digestion–ligation method, a lighting cloning system (BDIT0014, Biodragon Immunotechnology), or Gateway technology (Thermo Fisher). The coding sequences of genes were used for vector construction. For split luciferase assays, the genes were cloned into *Kpn I*/*Sal I*-digested *pJW771* or *pJW772* to generate Nluc and Cluc fusions, respectively; *RAD51* was cloned into *Nco I*/*Xba I*-digested *pFGC5941*. For protein expression in *Escherichia coli*, *SNI1* and *ASAP1* were inserted into *BamH I*/*Xho I*-digested *pGEX-6P-1* (GE Healthcare) to generate *GST-SNI1*/*ASAP1*; *RAD51* was cloned into *pDEST15* vector to generate *GST-RAD51*, and *DMC1* was cloned into *pDEST-HisMBP* to generate *HisMBP-DMC1*; *DMC1* and *RAD51* were inserted into *Nco I*/*Hind III*-digested *pET28a* (Merck) to generate *DMC1*/*RAD51*-His. For CoIP assays in Arabidopsis protoplast, *SNI1*, *ASAP1*, and *RAD51* were cloned into *Kpn I*/*BamH I*-digested *pM999* to generate *SNI1*/*ASAP1*/*RAD51-GFP*; *DMC1* and *RAD51* were cloned into *pUCGW14* to generate *DMC1*/*RAD51-HA* using Gateway technology. All primers used were listed in Supplemental Table S1.

Pull-down assays

The pull-down assays were performed as described previously (Wang et al., 2021). All proteins used were expressed in *E. coli BL21* (induced with 0.5 mM IPTG at 16°C for 14–16 h) and purified using glutathione-sepharose resin (CW0190S, CoWin Biosciences) or Ni-Agarose Resin (CW0010S, CoWin Biosciences). The GST-tagged proteins were coupled to glutathione beads and incubated with His-tagged proteins in binding buffer (140 mM NaCl, 2.7 mM KCl, 10 mM Na_2HPO_4, 1.8 mM KH_2PO_4, pH 7.4) for 2 h in 4°C. For competition pull-down assays, the purified protein of HisMBP-DMC1 coupled with amylose resin beads (SA026010, Smart Lifescience) was divided into three equal portions and incubated with the same amount of GST-SNI1 or GST-ASAP1 proteins but different amounts of RAD51-His proteins. The beads were then washed three times with washing buffer (140 mM NaCl, 2.7 mM KCl, 10 mM Na_2HPO_4, 1.8 mM KH_2PO_4, 1% Triton X-100, pH 7.4). The proteins were eluted by incubating beads with 2× Sodium Dodecyl Sulfate (SDS) loading buffer at 100°C for 8 min. Both the input and pull-down samples were subjected to immunoblotting using anti-GST (1:4,000, Promoter), anti-His (1:4,000, Promoter), and anti-MBP (1:4,000, AE016, ABclonal) antibodies.

Split luciferase assays

The split luciferase assays were performed as described (Chen et al., 2008). The Nluc or Cluc constructs were transformed into *Agrobacterium tumefaciens* strain GV3101, respectively. After induction using 150-μM acetosyringone for 2–3 h, the agrobacteria were infiltrated into *N. benthamiana* for transient expression. After 48 h of incubation, 1 mM luciferin was applied onto leaves and the images were

captured using Lumazone imaging system equipped with 2048B CCD camera (Roper). For competition split luciferase assays, *ASAP1/SNI1-Nluc* and *Cluc-DMC1* were co-expressed with either empty vector or *RAD51*.

CoIP assays

The CoIP assays were performed as described previously (Pan et al., 2021). The *DMC1-HA* was co-expressed with *SNI1-GFP*, *ASAP1-GFP*, *RAD51-GFP*, or *GFP* in Arabidopsis protoplasts. Total proteins were extracted using extraction buffer (100 mM Tris–HCl, pH 7.0, 150 mM NaCl, 0.1% Nonidet P 40, 1 mM PhenylMethaneSulfonyl Fluoride (PMSF), 1× protease inhibitor cocktail) and were precipitated by GFP-Trap-M (gtm-20, Chromotek) at 4°C for 3 h. The beads were washed using washing buffer (100 mM Tris–HCl, pH 7.0, 150 mM NaCl, 0.1% Nonidet P-40) five times and eluted by incubating with 2× SDS loading buffer at 100°C for 8 min. For the CoIP assay between RAD51-HA and SNI1-GFP or ASAP1-GFP, the same method as above was used. Both the input and immunoprecipitated samples were subjected to immunoblotting using anti-GFP (1:3,000, Promoter) or anti-HA (1:3,000, Promoter) antibodies.

Quantitative RT-PCR assays

Total RNA was isolated using Trizol Reagent according to manufacturer's protocol (RN0102, Aidlab). Reverse transcription reaction was performed using HiScriptII Q RT Supermix for qPCR with gDNA Eraser according to the manufacturer's protocol (R223-01, Vazyme). The qPCR assays were performed on the CFX Connect Real-Time PCR Detection System (Bio-Rad) using ChamQ Universal SYBR qPCR Master Mix (Q711-02, Vazyme). The *UBIQUITIN 5* (*UBQ5*) gene was used as a reference for gene expression in Arabidopsis. The *NbEF1α* gene was used as reference for gene expression in *N. benthamiana*. The relative expression level was calculated using the $2^{-\Delta\Delta CT}$ method. The primer sequences are listed in Supplemental Table S1.

Accession numbers

Sequence data from this article can be found in the Arabidopsis Genome Initiative or GenBank/EMBL databases under the following accession numbers: *DMC1* (At3g22880), *RAD51* (At5g20850), *SNI1* (At4g18470), *ASAP1* (At2g28130), *MMS21* (At3g15150), *ASY1* (At1g67370), and *ZYP1* (At1g22260).

Supplemental data

The following materials are available in the online version of this article.

Supplemental Figure S1. The point-mutation *sni1-1* mutant cannot suppress the sterility of *rad51* (Supports Figure 1).

Supplemental Figure S2. The T-DNA insertion *sni1-2* mutant is a null allele (Supports Figure 1).

Supplemental Figure S3. The *mms21* mutant suppresses the sterility of *rad51* (Supports Figure 1).

Supplemental Figure S4. Chromosome 1 painting and 45S rDNA FISH (Supports Figure 2).

Supplemental Figure S5. The relative expression levels of *SNI1*, *ASAP1*, and *DMC1* determined by RT-qPCR assays (Supports Figure 7).

Supplemental Table S1. All primers used in this study.

Acknowledgments

We thank Dr Chengwei Yang from South China Normal University for sharing the *mms21* mutant and Dr Tao Zhang from Yangzhou University for designing Chromosome 1 library for chromosome painting.

Funding

The work was supported by grants from the National Natural Science Foundation of China (grant no. 31771355 and 31970311 to S.Y., grant no. 31925005 to Y.W., grant no. 32000372 to X.W., and grant no. 31722017 to P.Y.), the Fundamental Research Funds for the Central Universities (grant no. 2662019PY029 to S.Y.), and the State Key Laboratory of Genetic Engineering, Fudan University to Y.W.

Conflict of interest statement. There is no conflict of interest.

References

Alexander MP (1969) Differential staining of aborted and nonaborted pollen. Stain Technol **44**: 117–122.

Aragón L (2018) The Smc5/6 complex: new and old functions of the enigmatic long-distance relative. Annu Rev Genet **52**: 89–107.

Armstrong SJ, Caryl AP, Jones GH, Franklin FCH (2002) Asy1, a protein required for meiotic chromosome synapsis, localizes to axis-associated chromatin in Arabidopsis and Brassica. J Cell Sci **115**: 3645–3655

Bergerat A, de Massy B, Gadelle D, Varoutas P-C, Nicolas A, Forterre P (1997) An atypical topoisomerase II from archaea with implications for meiotic recombination. Nature **386**: 414–417

Bishop DK (1994) RecA homologs Dmc1 and Rad51 interact to form multiple nuclear complexes prior to meiotic chromosome synapsis. Cell **79**: 1081–1092

Chan Y-L, Zhang A, Weissman BP, Bishop DK (2019) RPA resolves conflicting activities of accessory proteins during reconstitution of Dmc1-mediated meiotic recombination. Nucleic Acids Res **47**: 747–761

Chen H, Zou Y, Shang Y, Lin H, Wang Y, Cai R, Tang X, Zhou J-M (2008) Firefly luciferase complementation imaging assay for protein-protein interactions in plants. Plant Physiol **146**: 368–376

Chiolo I, Minoda A, Colmenares SU, Polyzos A, Costes SV, Karpen GH (2011) Double-strand breaks in heterochromatin move outside of a dynamic HP1a domain to complete recombinational repair. Cell **144**: 732–744

Cloud V, Chan YLY-L, Grubb J, Budke B, Bishop DK (2012) Rad51 is an accessory factor for Dmc1-mediated joint molecule formation during meiosis. Science **337**: 1222–1225

Copsey A, Tang S, Jordan PW, Blitzblau HG, Newcombe S, Chi-ho Chan A, Newnham L, Li Z, Gray S, Herbert AD, et al. (2013). Smc5/6 coordinates formation and resolution of joint molecules with chromosome morphology to ensure meiotic divisions. PLoS Genet **9**: e1004071

Couteau F, Belzile F, Horlow C, Grandjean O, Vezon D, Doutriaux MP (1999) Random chromosome segregation without meiotic

arrest in both male and female meiocytes of a dmc1 mutant of Arabidopsis. Plant Cell **11**: 1623–1634

de Massy B (2013) Initiation of meiotic recombination: How and where? Conservation and specificities among eukaryotes. Annu Rev Genet **47**: 563–599

Da Ines O, Degroote F, Goubely C, Amiard S, Gallego ME, White CI (2013) Meiotic recombination in Arabidopsis is catalysed by DMC1, with RAD51 playing a supporting role. PLoS Genet **9**: e1003787.

Díaz M, Pečinková P, Nowicka A, Baroux C, Sakamoto T, Gandha PY, Jeřábková H, Matsunaga S, Grossniklaus U, Pecinka A (2019) The SMC5/6 complex subunit NSE4A is involved in DNA damage repair and seed development. Plant Cell **31**: 1579–1597

Fukuda T, Alsheimer M, Llano E, Jordan PW, Gomez R, Pendas AM, Suja JA, Handel MA, Viera A, Jessberger R (2013) Dynamic localization of SMC5/6 complex proteins during mammalian meiosis and mitosis suggests functions in distinct chromosome processes. J Cell Sci **126**: 4239–4252

Grelon M (2001) AtSPO11-1 is necessary for efficient meiotic recombination in plants. EMBO J **20**: 589–600

Han Y, Zhang T, Thammapichai P, Weng Y, Jiang J (2015). Chromosome-specific painting in Cucumis species using bulked oligonucleotides. Genetics **200**: 771–779

Hazbun TR, Malmström L, Anderson S, Graczyk BJ, Fox B, Riffle M, Sundin BA, Aranda JD, McDonald WH, Chiu CH, et al. (2003). Assigning function to yeast proteins by integration of technologies. Mol Cell **12**: 1353–1365

Heyer W-DD, Ehmsen KT, Liu J (2010) Regulation of homologous recombination in eukaryotes. Annu Rev Genet **44**: 113–139

Higgins JD, Sanchez-Moran E, Armstrong SJ, Jones GH, Franklin FCH (2005) The Arabidopsis synaptonemal complex protein ZYP1 is required for chromosome synapsis and normal fidelity of crossing over. Genes Dev **19**: 2488–2500

Hinch AG, Becker PW, Li T, Moralli D, Zhang G, Bycroft C, Green C, Keeney S, Shi Q, Davies B, et al. (2020). The configuration of RPA, RAD51, and DMC1 binding in meiosis reveals the nature of critical recombination intermediates. Mol Cell **79**: 689–701

Huang J, Cheng Z, Wang C, Hong Y, Su H, Wang J, Copenhaver GP, Ma H, Wang Y (2015) Formation of interference-sensitive meiotic cross-overs requires sufficient DNA leading-strand elongation. Proc Natl Acad Sci USA **112**: 12534–12539

Huang L, Yang S, Zhang S, Liu M, Lai J, Qi Y, Shi S, Wang J, Wang Y, Xie Q, Yang C (2009) The Arabidopsis SUMO E3 ligase AtMMS21, a homologue of NSE2/MMS21, regulates cell proliferation in the root. Plant J **60**: 666–678

Keeney S (2001) Mechanism and control of meiotic recombination initiation. Curr Top Dev Biol **52**: 1–53

Kurzbauer M-T, Uanschou C, Chen D, Schlögelhofer P (2012) The recombinases DMC1 and RAD51 are functionally and spatially separated during meiosis in Arabidopsis. Plant Cell **24**: 2058–2070

Lan WH, Lin SY, Kao CY, Chang WH, Yeh HY, Chang HY, Chi P, Li HW (2020) Rad51 facilitates filament assembly of meiosis-specific Dmc1 recombinase. Proc Natl Acad Sci USA **117**: 2–9

Li W, Chen C, Markmann-Mulisch U, Timofejeva L, Schmelzer E, Ma H, Reiss B (2004) The Arabidopsis AtRAD51 gene is dispensable for vegetative development but required for meiosis. Proc Natl Acad Sci USA **101**: 10596–10601

Li X, Zhang YL, Clarke JD, Li Y, Dong XN (1999) Identification and cloning of a negative regulator of systemic acquired resistance, SNI1, through a screen for suppressors of npr1-1. Cell **98**: 329–339

Lilienthal I, Kanno T, Sjögren C (2013) Inhibition of the Smc5/6 complex during meiosis perturbs joint molecule formation and resolution without significantly changing crossover or non-crossover levels. PLoS Genet **9**: e1003898

Liu M, Shi S, Zhang S, Xu P, Lai J, Liu Y, Yuan D, Wang Y, Du J, Yang C (2014) SUMO E3 ligase AtMMS21 is required for normal meiosis and gametophyte development in Arabidopsis. BMC Plant Biol **14**: 153

Lysak M, Fransz P, Schubert I (2006) Cytogenetic analyses of Arabidopsis. Methods Mol Biol **323**: 173–186

Mercier R, Mézard C, Jenczewski E, Macaisne N, Grelon M (2015) The molecular biology of meiosis in plants. Annu Rev Plant Biol **66**: 297–327

Pan T, Qin Q, Nong C, Gao S, Wang L, Cai B, Zhang M, Wu C, Chen H, Li T, et al. (2021). A novel WEE1 pathway for replication stress responses. Nat Plants **7**: 209–218

Pebernard S, Wohlschlegel J, McDonald WH, Yates JR, Boddy MN, Yates JR3rd Boddy, MN (2006) The Nse5-Nse6 dimer mediates DNA repair roles of the Smc5-Smc6 complex. Mol Cell Biol **26**: 1617–1630

Potts PR (2009) The Yin and Yang of the MMS21-SMC5/6 SUMO ligase complex in homologous recombination. DNA Repair **8**: 499–506

Pradillo M, Varas J, Oliver C, Santos JL (2014) On the role of AtDMC1, AtRAD51 and its paralogs during Arabidopsis meiosis. Front Plant Sci **5**: 23

Raschle M, Smeenk G, Hansen RK, Temu T, Oka Y, Hein MY, Nagaraj N, Long DT, Walter JC, Hofmann K, et al. (2015) Proteomics reveals dynamic assembly of repair complexes during bypass of DNA cross-links. Science **348**: 1253671–1253671.

Reitz D, Grubb J, Bishop DK (2019) A mutant form of Dmc1 that bypasses the requirement for accessory protein Mei5-Sae3 reveals independent activities of Mei5-Sae3 and Rad51 in Dmc1 filament stability. PLOS Genet **15**: e1008217

Robert T, Nore A, Brun C, Maffre C, Crimi B, Guichard V, Bourbon HM, de Massy B (2016) The TopoVIB-Like protein family is required for meiotic DNA double-strand break formation. Science **351**: 943–949

Tarsounas M, Morita T, Pearlman RE, Moens PB (1999) RAD51 and DMC1 form mixed complexes associated with mouse meiotic chromosome cores and synaptonemal complexes. J Cell Biol **147**: 207–219

Uhlmann F (2016) SMC complexes: from DNA to chromosomes. Nat Rev Mol Cell Biol **17**: 399–412

Verver DE, Hwang GH, Jordan PW, Hamer G (2016) Resolving complex chromosome structures during meiosis: versatile deployment of Smc5/6. Chromosoma **125**: 15–27

Verver DE, Langedijk NSM, Jordan PW, Repping S, Hamer G (2014) The SMC5/6 complex is involved in crucial processes during human spermatogenesis1. Biol Reprod **91**: 1–10

Vignard J, Siwiec T, Chelysheva L, Vrielynck N, Gonord F, Armstrong SJ, Schlögelhofer P, Mercier R (2007) The interplay of RecA-related proteins and the MND1–HOP2 complex during meiosis in Arabidopsis thaliana. PLoS Genet **3**: e176

Vrielynck N, Chambon A, Vezon D, Pereira L, Chelysheva L, De Muyt A, Mezard C, Mayer C, Grelon M (2016) A DNA topoisomerase VI-like complex initiates meiotic recombination. Science **351**: 939–943

Wang H, Xu W, Sun Y, Lian Q, Wang C, Yu C, He C, Wang J, Ma H, Copenhaver GP, et al. (2020) The cohesin loader SCC2 contains a PHD finger that is required for meiosis in land plants. PLOS Genet **16**: e1008849

Wang L, Zhan L, Zhao Y, Huang Y, Wu C, Pan T, Qin Q, Xu Y, Deng Z, Li J, et al. (2021) The ATR-WEE1 kinase module inhibits the MAC complex to regulate replication stress response. Nucleic Acids Res **49**: 1411–1425

Wang L, Chen H, Wang C, Hu Z, Yan S (2018) Negative regulator of E2F transcription factors links cell cycle checkpoint and DNA damage repair. Proc Natl Acad Sci USA **115**: E3837–E3845

Wang S, Durrant WE, Song J, Spivey NW, Dong X (2010) Arabidopsis BRCA2 and RAD51 proteins are specifically involved in defense gene transcription during plant immune responses. Proc Natl Acad Sci USA **107**: 22716–22721

Wang Y, Cheng Z, Lu P, Timofejeva L, Ma H (2014) Molecular cell biology of male meiotic chromosomes and isolation of male meiocytes in Arabidopsis thaliana. In José Luis Riechmann and Frank

Wellmer, eds Methods in Molecular Biology, Springer New York, NY, pp 217–230

Wang Y, Copenhaver GP (2018) Meiotic recombination: mixing it up in plants. Annu Rev Plant Biol **69**: 577–609

Wehrkamp-Richter S, Hyppa RW, Prudden J, Smith GR, Boddy MN (2012) Meiotic DNA joint molecule resolution depends on Nse5-Nse6 of the Smc5-Smc6 holocomplex. Nucleic Acids Res **40**: 9633–9646

Xaver M, Huang L, Chen D, Klein F (2013) Smc5/6-Mms21 prevents and eliminates inappropriate recombination intermediates in meiosis. PLoS Genet **9**: e1004067

Yan S, Wang W, Marqués J, Mohan R, Saleh A, Durrant WE, Song J, Dong X (2013) Salicylic acid activates DNA damage responses to potentiate plant immunity. Mol Cell **52**: 602–610

Yao Y, Li X, Chen W, Liu H, Mi L, Ren D, Mo A, Lu P (2020) ATM promotes RAD51-mediated meiotic DSB repair by inter-sister-chromatid recombination in Arabidopsis. Front Plant Sci **11**: 839

Zelkowski M, Zelkowska K, Conrad U, Hesse S, Lermontova I, Marzec M, Meister A, Houben A, Schubert V (2019) Arabidopsis NSE4 proteins act in somatic nuclei and meiosis to ensure plant viability and fertility. Front Plant Sci **10**: 774